Hindawi
Advances in Materials Science and Engineering
Volume 2021, Article ID 4732799, 11 pages
https://doi.org/10.1155/2021/4732799

Research Article

Effects of Hydrated Lime on High-Temperature Rheological Properties of High-Viscosity Modified Asphalt

Wenjing Zhou,[1,2] **Yihan Sun**,[1,2] **Fengxia Chi**,[1,2] **Qinling Cheng**,[1,2] **and Bo Han**[1,2]

[1]*Zhejiang Key Laboratory of Road and Bridge Detection and Maintenance Technology, Hangzhou 311305, China*
[2]*Zhejiang Academy of Transportation Sciences, Hangzhou 310023, China*

Correspondence should be addressed to Yihan Sun; sunyh@whut.edu.cn

Received 16 July 2021; Revised 3 September 2021; Accepted 4 September 2021; Published 6 October 2021

Academic Editor: Tomasz Trzepieciński

High-viscosity modified asphalt (HVA) is widely used as the binder for permeable asphalt pavement, and hydrated lime (HL) attracts a strong technical interest as an effective moisture additive in asphalt for a long time. However, the application of HL in HVA has been rarely studied. The present study evaluates the influence of HL on the high-temperature rheological properties of HVA and selects the optimum HL content and fineness. The asphalt mortars of HVA and HL of different contents and fineness were prepared. Temperature scanning (DSR-TS), multiple stress creep recovery (MSCR) by using a dynamic shear rheometer, and scanning electron microscope (SEM) tests were carried out to evaluate the high-temperature rheological properties and microstructure morphology characteristics of the asphalt mortars. Based on the DSR-TS and MSCR tests, the results showed that high-temperature performance together with the ability to deformation resistance of HVA was improved apparently with the increase of the HL content. When the HL content is above 1.2, the stress sensitivity of HVA is lower. The SEM results clearly showed that the uniformity of asphalt mortars could be effectively guaranteed when the HL content was 1.2 and the fineness was 800 mesh. The HL fineness has little effect on the high-temperature performance of HVA. In summary, taking into account the high-temperature performance and microstructure of HVA with HL, the optimum HL content and fineness could be finally determined.

1. Introduction

An asphalt mixture comprises a three-phase inhomogeneous material matrix, including asphalt binder, graded mineral aggregates, and air voids [1, 2]. As an important component of pavement material, the properties of the asphalt binder play a vital role in affecting the pavement performance [3, 4]. In China, due to the heavy traffic axle load and the complete climate environment, high-viscosity modified asphalt (HVA) is commonly used as the asphalt binder to increase the performance of the porous asphalt mixture for the drainage asphalt pavement, which solves the problems of scattering and spalling when using ordinary modified asphalt to build the drainage asphalt pavement [5]. HVA is a kind of polymer modified asphalt with high molecular amount, which is composed of thermoplastic rubber, resin, antiaging agent, and plasticizer. The Japanese standard set a standard that the dynamic viscosity of HVA at 60°C should be greater than 2×10^4 Pa·s, and softening point should be greater than 80°C [6].

Although known for a long time, hydrated lime (HL) still attracts a strong technical interest as an asphalt additive [6, 7], with the advantages of resisting moisture damage and improving the modulus, strength, rutting resistance, fatigue, and thermal stability of asphalt [8, 9]. HL is a well-known material for improving the resistance against moisture and frost damage of asphalt mixtures in which its application dates back to the 1970s [10–12]. HL composed of calcium hydroxide $Ca(OH)_2$ can accumulate calcium ions on the aggregate surface. When the aggregate surface is humid or the water content in the air is high, HL reacts with water and carbon dioxide in the air to form calcium carbonate, which makes the aggregate and asphalt have a stronger adhesion and resist the water damage of the asphalt mixture [13].

Therefore, for the drainage pavement, adding HL into HVA can improve the adhesion, water damage resistance, and durability of the asphalt mixture.

Various studies [14–17] have been performed on the effect of HL on the main engineering properties of asphalt mixtures and revealed that stiffness, resistance against cracking, rutting, and ageing are improved. Han et al. [18, 19] evaluated the adhesion between base asphalt and HL by the surface free energy method. Some laboratory findings and field studies have manifested that HL increases pavement durability [20–22]. Rasouli et al. determined the fatigue behavior of asphalt mixtures with HL and found that replacement of the aggregate filler with HL could increase the flexural stiffness of asphalt mixtures [11, 23]. The linear viscoelastic characteristics and fatigue properties of asphalt mixtures containing HL [24] showed that HL can increase complex modulus of mixtures; however, it does not change the fatigue properties of mixtures. Zhu et al. [25] studied the influence of limestone powder on the viscoelastic mechanical properties of HVA mortar and found that mineral powder can stiffen the asphalt binder and improve the high-temperature deformation resistance of the mortar. Xing et al. [26] found that increasing the viscosity of asphalt or increasing the specific surface area of the mineral powder can effectively reduce the temperature sensitivity of HVA and resist the high-temperature deformation of HVA. Mo et al. [27] compared the influence of HL and cement on the fatigue performance of asphalt mortar and obtained that the fatigue performance of HL and cement is better than limestone.

In summary, the aforementioned studies demonstrated the positive effect of HL on the properties of asphalt mixtures in three ways: by resisting to stripping, improving the resistance to permanent deformation, and increasing the flexural stiffness. However, most of the current research studies focus on the influence of HL on the base asphalt binder and asphalt mixtures, and some of them study the influence of the limestone powder on the properties of HVA. In order to implement the actual application of HL in HVA of the drainage asphalt pavement, the high-temperature rheological properties and microstructure tests were conducted to study on the effect of the content and fineness of HL on HVA. The results of this research also extended the knowledge on the properties of HVA modified by HL.

2. Materials and Methods

2.1. Materials

2.1.1. HVA. HVA used in this paper is rubber powder/SBS composite modified asphalt, and the conventional tests are performed following the Chinese standard [28, 29], and the results are shown in Table 1.

2.1.2. HL. Three kinds of HL with different particle sizes from the same origin were used in this study. The basic characterizations were carried out using the X-ray fluorescence spectrometer, laser particle size analyzer, BET-specific surface analyzer (Table 2), and SEM imaging. It can be seen from Table 3 that the oxides of HL are mainly composed of CaO and SiO_2. Figure 1 shows the particle size distribution of HL, where 400 mesh ranges from 0.4 to 500 μm, 600 mesh from 0.4 to 75 μm, and 800 mesh from 0.4 to 45 μm. The SEM image of all HL is shown in Figure 2. It can be seen that the HL fillers are block in shape and have rugose surface texture, and there was no agglomeration between particles.

Table 1: Main performance of asphalt.

Performance metrics	The test value
Penetration (25°C, 100 g, 5 s) (0.1 mm)	29.3
Ductility (25°C, 5 cm/min) (cm)	20.0
Softening point (ring-and-ball method) (°C)	81.8
Elastic recovery (25°C) (%)	72.7
Rotational viscosity (190°C) (Pa·s)	2.2
Dynamic viscosity (60°C) (Pa·s)	50468

2.2. Sample Preparation. HVA was modified with 400 mesh, 600 mesh, and 800 mesh HL, and the HL content of every kind of mesh comprised 0.6, 0.9, 1.2, and 1.5 by the mass ratio of HL to HVA.

By preparing asphalt mortar, the HVA was first heated at 175–185°C for about 1 h to melt. Then, HL which was kept at 175°C–185°C for 30–45 min was added into the hot HVA. Finally, they were mixed by using a high-shear mixer rotating at 400–600 r/min for 120 min at 180°C. After that, the preparation of samples has been finished.

The meaning of the sample number followed in this paper is explained such that asphalt mortar #0 (AM0) represents HVA, and asphalt mortar #1 (AM1), asphalt mortar #2 (AM2), asphalt mortar #3 (AM3), and asphalt mortar #4 (AM4) represent that HVA was prepared with HL (400 mesh) at different contents (0.6, 0.9, 1.2, and 1.5) of the mass ratio of HL to HVA, respectively. Asphalt mortar #5 (AM5) and asphalt mortar #6 (AM6) represent HVA mixed with 600 mesh and 800 mesh HL, and the ratio is 1.2.

2.3. Test Methods

2.3.1. Dynamic Shear Rheometer for Temperature Scanning (DSR-TS) and Multiple Stress Creep Recovery (MSCR) Tests. The equipment for the DSR-TS and MSCR [30, 31] tests is Anton Paar CTD180 used by the 25 mm parallel plate rotor.

(1) DSR-TS test: DSR-TS test was applied over the range of 30°C–160°C at the strain of 0.5% and the frequency of 10 rad/s in the strain-control mode. The heating rate was set to 1°C/min.

(2) MSCR test: MSCR test was conducted to test the elastic recovery behavior and stress-dependent behavior of different asphalt mortars at 76°C under 0.1 kPa and 3.2 kPa creep stress, respectively, in accordance with AASHTO T350-14 [32]. During the test, the shear stress of 0.1 kPa was used to load for 1 s duration creep followed with a stress recovery for 9 s duration. Each stress cycle of every asphalt mortar experiences a creep recovery process for a total of 20 cycles. The strain reaches the peak value ε_c at the end of the creep phase. The strain recovered at the end of the period is

Table 2: Specific surface area of HL.

Sample name	400 mesh	600 mesh	800 mesh
Specific surface area (m^2/g)	1.2567	1.4988	1.9140

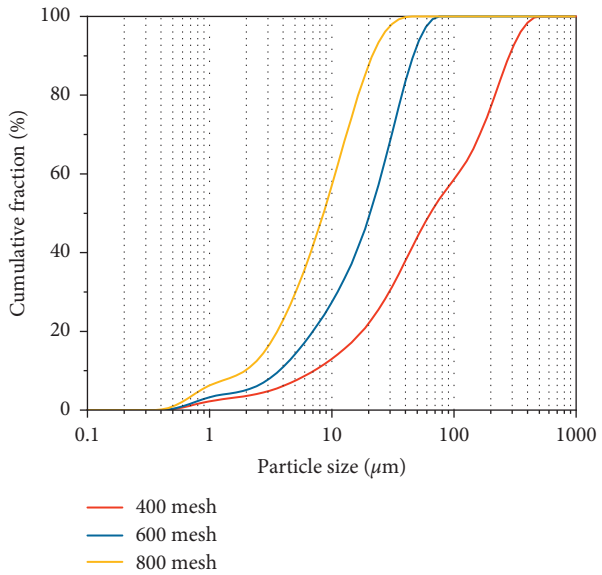

Figure 1: Particle size distribution curve of HL.

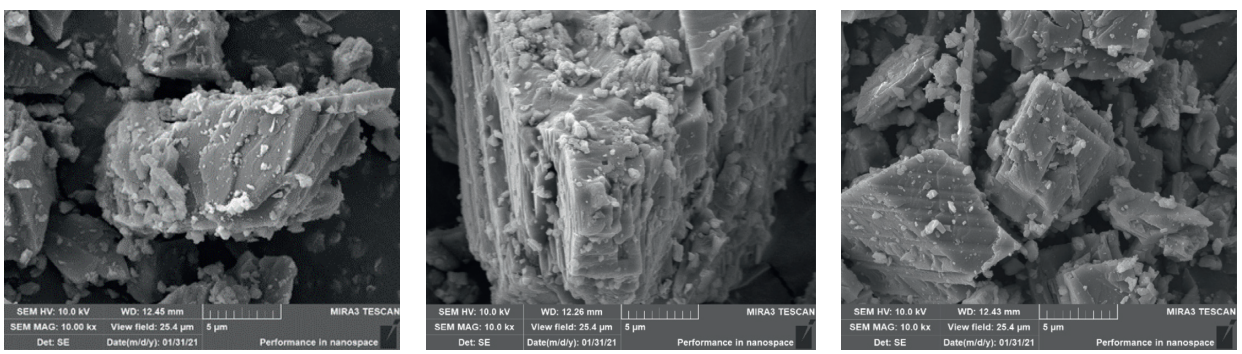

(a) (b) (c)

Figure 2: SEM imaging of HL at a zoom level of 10,000X. (a) 400 mesh. (b) 600 mesh. (c) 800 mesh.

Table 3: Oxide composition of HL.

Chemical composition (%) (mass)	400 mesh	600 mesh	800 mesh
CaO	78.1243	93.7304	96.7812
SiO_2	9.7359	5.2308	1.9839
Al_2O_3	0.4064	0.0479	0.0865
Fe_2O_3	0.3370	0.0846	0.0797
MgO	11.0640	0.7850	0.9611
SO_3	0.0781	0.0607	0.0549
K_2O	0.0462	—	—
P_2O_5	0.0182	—	—
MnO	0.1423	—	—
SrO	0.0476	0.0605	0.0528

ε_r. The irrecoverable strain is ε_u. The irrecoverable strain will continue to accumulate to the next cycle.

The average recovery rate R and the average irrecoverable creep compliance J_{nr} at the creep stress of 0.1 kPa and 3.2 kPa were calculated after every 10 creep and recovery cycles, as shown in formulae (1) and (4).

$$R_{0.1} = \frac{\mathrm{SUM}\left[\varepsilon_r(0.1, N)\right]}{10}, \quad \text{for } N = 1 \text{ to } 10, \tag{1}$$

$$R_{3.2} = \frac{\mathrm{SUM}\left[\varepsilon_r(3.2, N)\right]}{10}, \quad \text{for } N = 1 \text{ to } 10, \tag{2}$$

$$J_{nr_{0.1}} = \frac{\mathrm{SUM}\left[J_{nr}(0.1, N)\right]}{10}, \quad \text{for } N = 1 \text{ to } 10, \tag{3}$$

$$J_{nr_{3.2}} = \frac{\mathrm{SUM}\left[J_{nr}(3.2, N)\right]}{10}, \quad \text{for } N = 1 \text{ to } 10, \tag{4}$$

where N in the formula is the number of loading cycles.

2.3.2. SEM Test. The dispersing effect of different HL on HVA was evaluated by the SEM. Asphalt mortar samples were cut to the required size and adhered to the sample holder. After gold plating, the samples were placed in the SEM for scanning and photographing. The SEM instrument used was MIRA3 TESCAN. The voltage of this test was 10.0 kV, and the resolution was 20 μm.

The experimental framework of this paper is summarized in Figure 3.

3. Results and Discussion

3.1. DSR-TS Test Results

3.1.1. Influence of the HL Content. Figure 4 shows that the phase angle (δ) of asphalt mortars changes in three ways with the increase of temperature. At 30°C–60°C, δ decreases with the increase of temperature. δ of asphalt mortar with different contents of HL varies greatly. At the same temperature, δ of AM3 is the largest, and δ of others increases with the increase of the HL content. This is because the asphalt mortar has not been transformed into a fluid at 30°C–60°C, and the resistance of asphalt mortar to deformation increases with the addition of HL. At 60°C–120°C, δ of asphalt mortar with different contents of HL increases linearly with the increase of temperature. δ of samples AM1, AM2, AM3, and AM4 is less susceptible to the changes of the HL content. This result shows that the HVA in the mortar is mainly viscous, and the influence of the HL content on the viscosity is very small at 60°C–120°C. When the temperature exceeds 120°C, δ shows a decreasing trend with the rise in temperature. δ of HVA decreases obviously at 120°C, which of asphalt mortars decreases at about 135°C. At the same temperature, δ of asphalt mortars increases with the increase of the HL content. This result shows that the HL content improves the high-temperature stability of HVA. It was in agreement with the conclusion that HL could raise the asphalt viscosity and stiffen asphalt [19].

As can be seen from Figure 5, the change trend of the complex shear modulus (G^*) with temperature of four kinds of asphalt mortars is similar, and G^* decreases with the increase of temperature. At 30°C–60°C, when the HL content is less than 1.2, G^* increases with the increase of the HL content, and when the HL content increases to 1.5, G^* of AM4 is slightly lower than AM3. When the temperature is above 60°C, G^* of different asphalt mortars increases with the increase of the HL content. At the same temperature, G^* of asphalt mortars is greater than HVA and increases with the increase of the HL content.

The rutting factor index ($|G^*|/\sin\delta$) results of the asphalt mortars are illustrated in Figure 6. It can be seen from Figure 6 that the changes of $|G^*|/\sin\delta$ show a downward trend with the increase of temperature. At 30°C–60°C, $|G^*|/\sin\delta$ increases with the increase of the HL content when below 1.2, and $|G^*|/\sin\delta$ of AM4 is slightly lower than AM3. When the temperature is above 60°C, $|G^*|/\sin\delta$ increases with the increase of the HL content.

The addition of HL has a contribution in increasing the high-temperature performance of HVA. The reason for the above phenomenon is that, with the increase of the HL content, the solid composition in the binder increases, which increases the viscosity of the asphalt mortars, reduces the flow deformation at high temperature, and enhances the antirutting ability. This result is in accordance with the other references, which examine the influence of various types of mineral fillers on the rheological properties of the asphalt [32, 33].

3.1.2. Influence of HL Fineness. It can be seen from Figure 7 that, at 30°C–60°C, δ of three kinds of asphalt mortar decreases with the increase of temperature and increases with the increase of HL fineness. At 60°C–135°C, the variation of δ is similar. When the temperature is higher than 135°C, δ of asphalt mortars decreases with the increase of temperature, and the larger the particle size of HL is, the larger δ of asphalt mortar is. Analysis of the reasons for the above phenomenon may be that, at 30°C–60°C, the larger the mesh of HL is, the more uniform the asphalt mortar is, and its elastic performance is better, which is consistent with the microstructure obtained from the following SEM test results. With the increase of temperature, the mortar softens gradually, and the viscous component of HVA in the mortar increases, and the fineness of HL cannot change the proportion of the viscoelastic component of the HVA itself. Above 135°C, the asphalt mortar becomes fluid, and the surface of HVA and HL contacts fully, which improves the viscosity of asphalt mortars.

As can be seen from Figures 8 and 9, after adding HL of different fineness, G^* and $|G^*|/\sin\delta$ of the three asphalt mortars are less distinctive, indicating that the HL fineness has less effect on the high-temperature performance.

3.2. MSCR Test

3.2.1. Influence of the HL Content. Figures 10 and 11 show the time-strain curve by the MSCR test of asphalt mortars with different HL contents under 0.1 kPa and 3.2 kPa loading

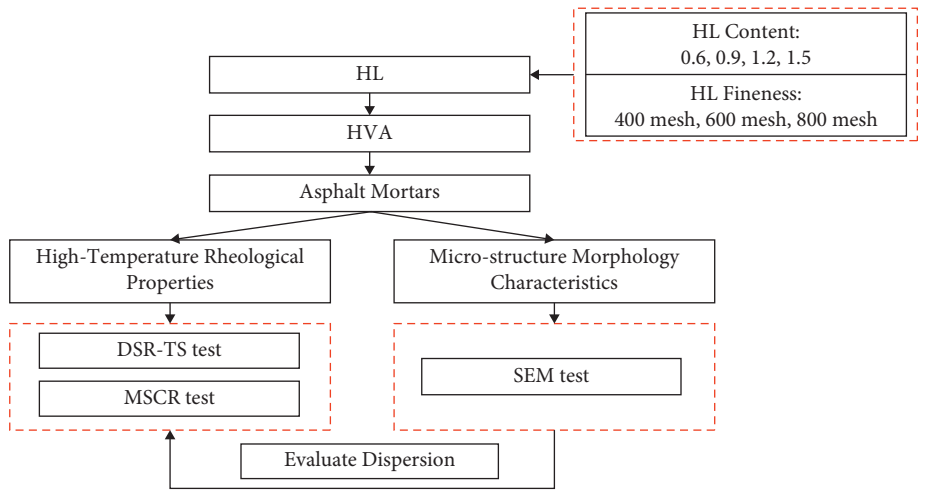

Figure 3: Flowchart of the research approach.

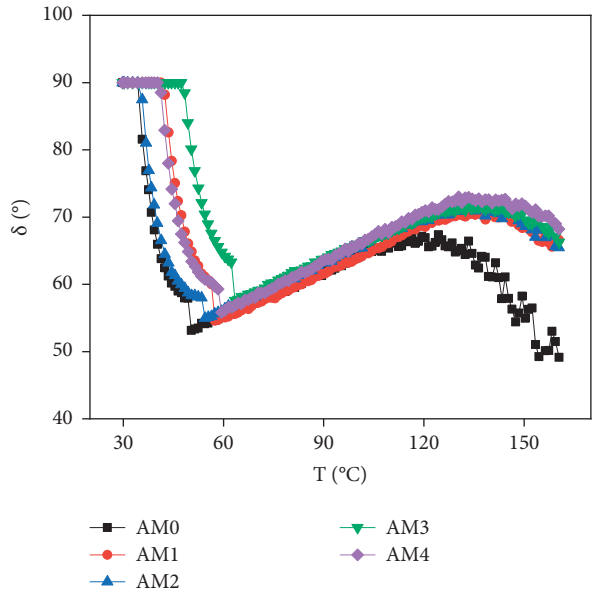

Figure 4: Change of δ of the asphalt mortar with temperature.

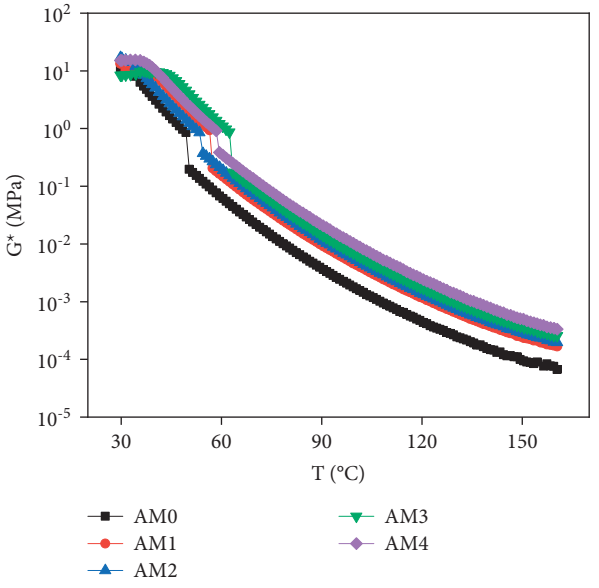

Figure 5: Change of complex shear modulus of the asphalt mortar with temperature.

conditions at 76°C. As illustrated by Figure 10, the larger the HL content is, the smaller the shear strain of asphalt mortar is. With the increase of loading time, the shear strain of HVA increases rapidly, where the increasing trend of asphalt mortars slows down, which indicates that HL improves the long-term deformation resistance of HVA. It can be seen from Figure 10 that the shear strain change of asphalt mortars decreases obviously after adding HL, and the larger the content is, the smaller the shear strain value is. Among them, the strain values of AM3 and AM4 are similar, far less than AM0. According to the research results of [16, 34, 35], the reason for this phenomenon may be that when the HL content is greater than 1.0, the particle-particle interaction and filler-bitumen interaction start to dominate the rheological behavior of the asphalt mortars, and the content of free asphalt in mortars decreases. And it is consistent with the microstructure of the SEM test below. Thus, further increase in the HL content led to almost no change in deformation. With the extension of time, the shear strain of AM0 increases rapidly, the shear strain of AM1 and AM2 slows down, and the shear strain of AM3 and AM4 tends to be linear.

The results of the average irrecoverable creep compliance (J_{nr}) of the five kinds of asphalt mortars with different HL contents are shown in Figure 12. It can be seen that, under 0.1 kPa and 3.2 kPa loading conditions, J_{nr} of asphalt mortars decreases significantly, indicating that the irrecoverable deformation decreases, and HL enhances the elastic deformation ability of HVA. Thus, the ability to resist permanent deformation at high temperature is improved. This is consistent with previous studies with respect to the effect of HL or other mineral fillers on the ability to resist permanent deformation of base asphalt by the MSCR test

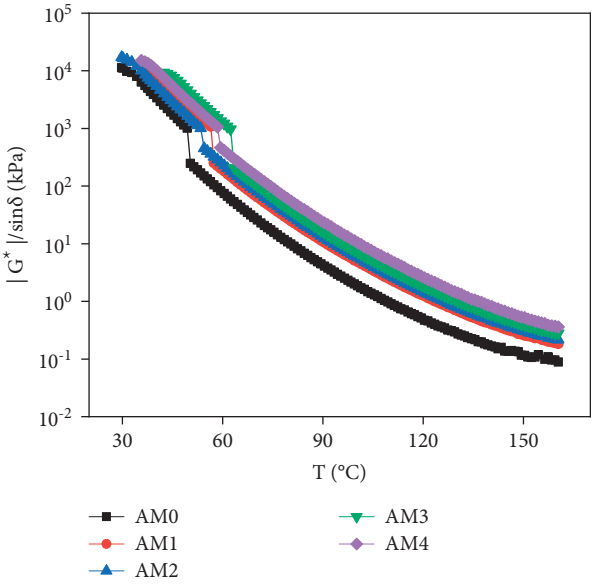

Figure 6: Change of the rutting factor of the asphalt mortar with temperature.

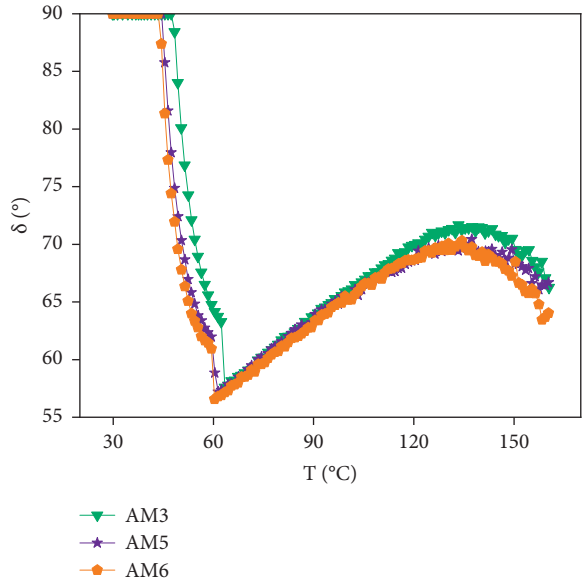

Figure 7: Change of δ of the asphalt mortar with temperature.

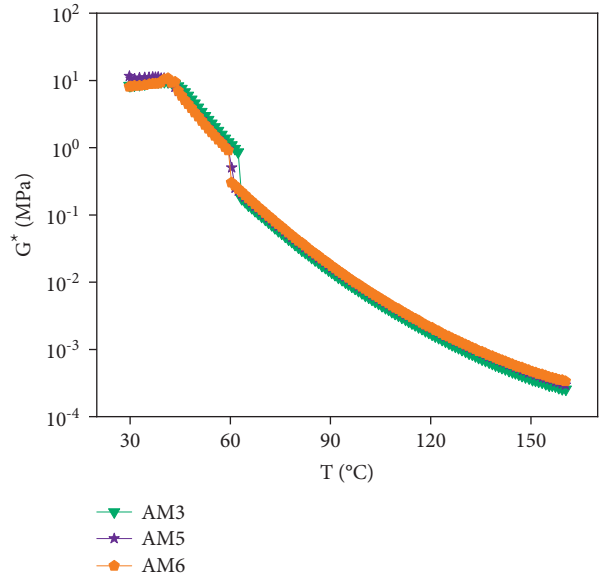

Figure 8: Change of complex shear modulus of the asphalt mortar with temperature.

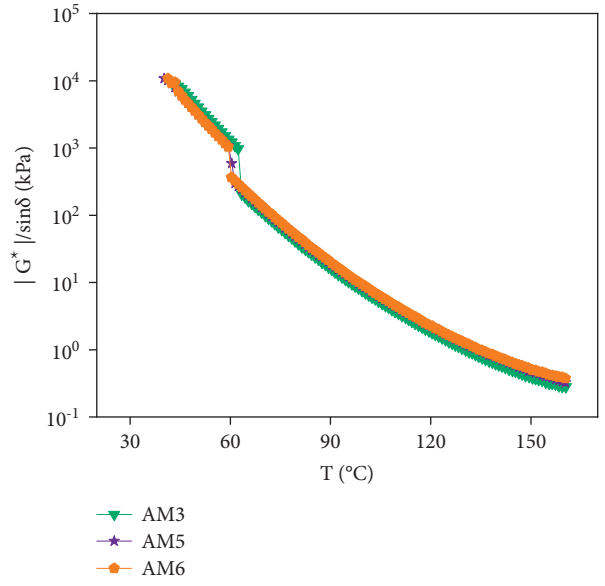

Figure 9: Change of the rutting factor of the asphalt mortar with temperature.

[11, 19, 32]. The comparative analysis shows that J_{nr} of AM1 and AM2 under 0.1 kPa is less than that of 3.2 kPa, and J_{nr} of AM3 and AM4 at 0.1 kPa is greater than that of 3.2 kPa, which indicates that when the HL content is above 1.2, the HVA can bear high-stress load better, and its stress sensitivity is lower.

The results of the average deformation recovery rate (R) of the asphalt mortars under two stress levels are shown in Figure 13. It can be found that the R values of HVA and asphalt mortars with different HL contents are similar under the 0.1 kPa stress level, which shows that the addition of HL does not change the dominant position of HVA on the elastic recovery performance of mortar. When the stress increases to 3.2 kPa, the R values of asphalt mortars decrease. When the content reaches 1.2, the R value of asphalt mortar is the largest, indicating that AM3 has the stronger anti-deformation ability.

3.2.2. Influence of HL Fineness. The time-strain change measured by the MSCR test with different HL fineness is shown in Figures 14 and 15. It can be seen that the shear strain of asphalt mortars decreases with the decrease of HL fineness under the low stress level. Under the high stress

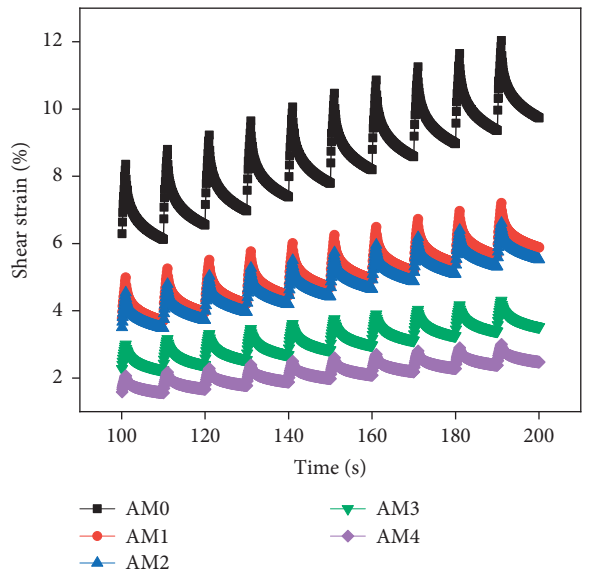

Figure 10: Strain-time diagram of the asphalt mortar at 0.1 kPa.

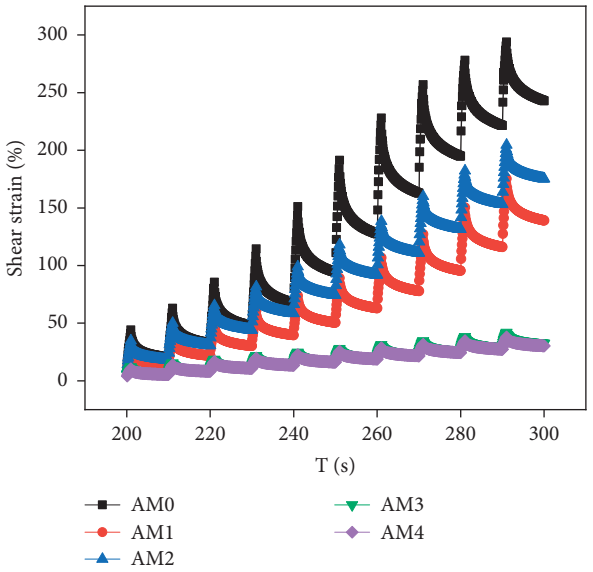

Figure 11: Strain-time diagram of the asphalt mortar at 3.2 kPa.

level, the shear strain curves of AM3 and AM6 coincide with each other, while the shear strain of AM5 is larger than that of AM3 and AM6.

Figure 16 shows the average irrecoverable creep compliance (J_{nr}) of the three kinds of asphalt mortars with different HL fineness. It is found that J_{nr} of AM6 is lower than that of AM3 under the 0.1 kPa stress level, and J_{nr} of AM3 and AM6 under the 3.2 kPa stress level is lower than 0.1 kPa, which indicates that the high-temperature anti-rutting performance of asphalt mortars is improved after adding 800 mesh HL. The results inferred that finer HL particle size can have a strong particle interaction with asphalt, which showed a considerable increase in the fatigue resistance ability of the asphalt mortar [35].

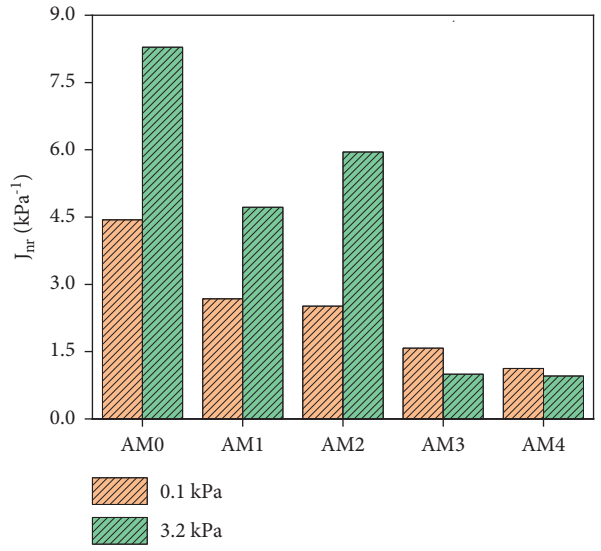

Figure 12: J_{nr} of the asphalt mortar at two stress levels.

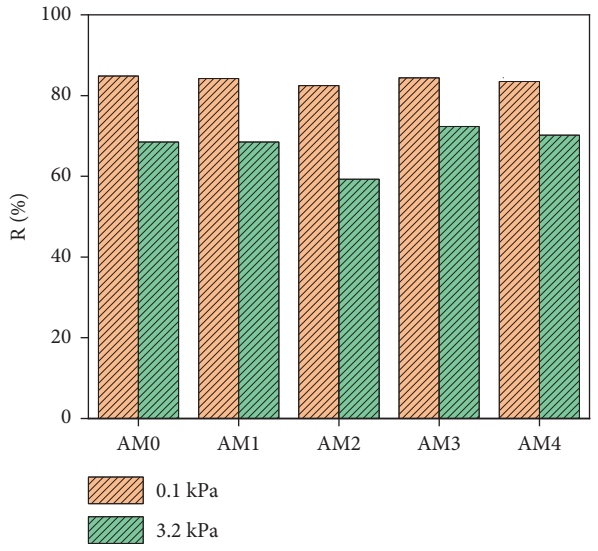

Figure 13: R of the asphalt mortar at two stress levels.

The results of the average deformation recovery rate (R) of AM3, AM5, and AM6 are shown in Figure 17. It can be found that the R values of asphalt mortars with different HL fineness are less distinctive, which indicates that the HL fineness has little effect on the elastic recovery performance of asphalt mortars.

3.3. Effect of HL on the Microstructure of HVA. In order to explore the dispersion of HL in HVA and the interface state of different phases between the two of them, the SEM test was carried out on the asphalt mortar specimens, and the results are shown in Figure 18. It can be seen from Figures 18(a)–18(d) that, at a magnification of the 20-time level, when the HL content is from 0.6 to 1.5, the microstructure of HVA and HL changes. The asphalt in AM1 basically completely encapsulates HL. With the increase of

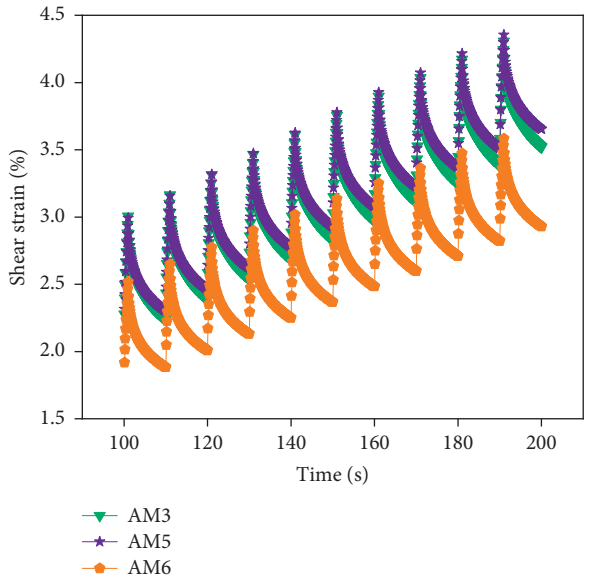

Figure 14: Strain-time diagram of the asphalt mortar at 0.1 kPa.

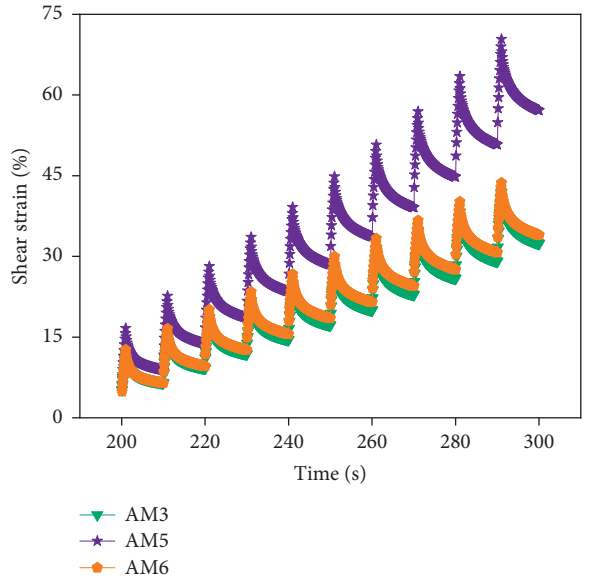

Figure 15: Strain-time diagram of the asphalt mortar at 3.2 kPa.

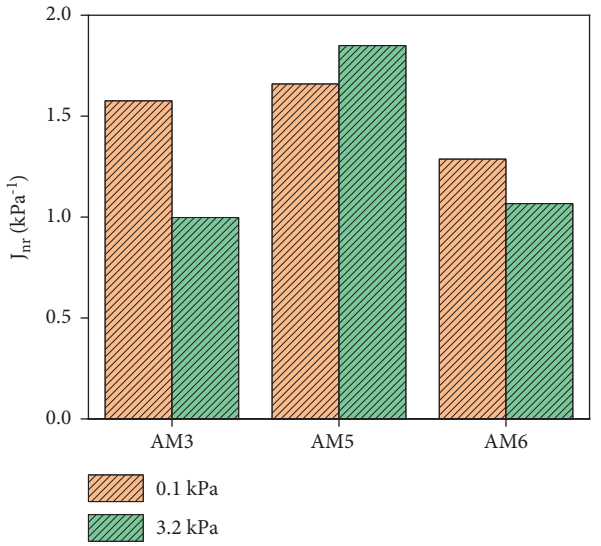

Figure 16: J_{nr} of the asphalt mortar at two stress levels.

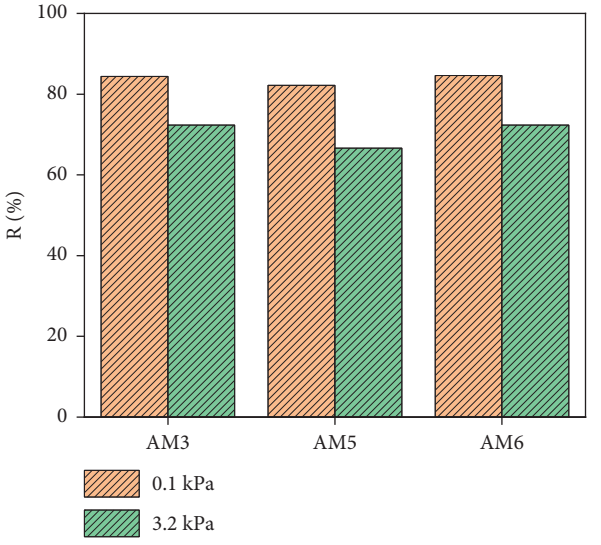

Figure 17: R of the asphalt mortar at two stress levels.

the HL content, part of HL is wrapped by asphalt and part of the surface is exposed outside the asphalt film which are beneficial to improve the strength and modulus of asphalt mortars. Other studies [36, 37] have found that the inorganic components such as mineral fillers enhance the elastic property of the neat asphalt and increase the rutting resistance of the asphalt at high temperatures, which is consistent with the conclusions of DSR-TS and MSCR tests above. When the HL content increases to 1.5, the agglomeration of HL can be seen. This is mainly because with the excessive increase of HL, it is difficult to well distribute into asphalt, resulting in the agglomeration of HL, which is not conducive to the performance of asphalt mortars. Therefore, when the HL content is 1.2, the dispersion of HVA with HL is better.

Compared with AM3, AM5, and AM6, when the HL fineness decreases, enlarging the surface area of HL particles, the surface bonding state of HVA and HL is more uniform. As is shown in Figures 18(d)–18(f), the exposed part of HL is less, which indicates that reducing the HL fineness can improve the dispersion uniformity of the asphalt binder.

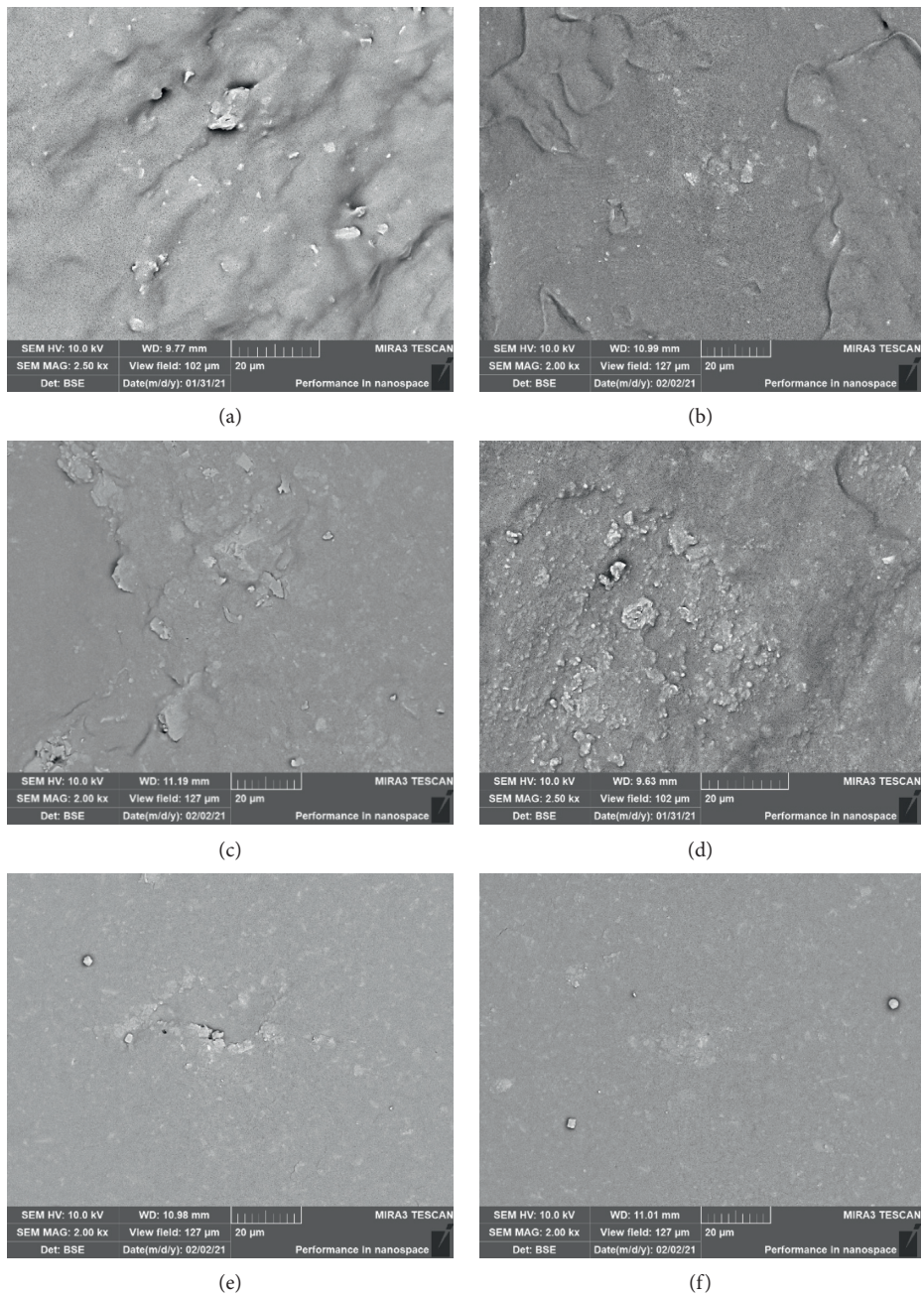

Figure 18: Microstructures of asphalt mortars. (a) AM1. (b) AM2. (c) AM3. (d) AM4. (e) AM5. (f) AM6.

4. Conclusion

In this study, the asphalt mortars made of HVA and HL were modified with different HL contents and fineness. The laboratory study evaluates the high-temperature rheological properties and microstructure of the asphalt mortar using DSR-TS, MSCR, and SEM tests. Based on the result outcomes, the following conclusions could be drawn:

(1) HL content played a leading role in the high-temperature performance of HVA. With the increase of the HL content, the high-temperature deformation resistance of HVA is enhanced. In the middle- and high-temperature region, the addition of HL has little effect on the viscosity of HVA. When the temperature rises above 120°C, the HL content has a greater effect on the viscoelasticity of HVA. The HL fineness has little effect on the high-temperature performance of HVA.

(2) With the increase of the HL content, the strain of asphalt mortars decreases, the deformation rate slows down, and the ability to resist permanent deformation increases. When the content is above 1.2, the stress sensitivity of HVA is lower, and its ability to resist deformation is stronger. The HL

fineness has no effect on the elastic recovery performance of asphalt.

(3) SEM test was used to characterize the dispersion effect of HVA with HL. It was found that the uniformity of asphalt mortars could be effectively guaranteed when the HL content was 1.2 and the fineness was 800 mesh.

(4) In this study, taking into account the high-temperature rheological properties and dispersion effect of HVA modified with HL, the optimum HL content and fineness were around 1.2 and 800 mesh, respectively.

Data Availability

The data used to support the findings of this study are available from the corresponding author upon request.

Conflicts of Interest

The authors declare that they have no conflicts of interest.

Authors' Contributions

Wenjing Zhou developed the methodology, wrote the original draft, contributed to project administration, and supervised the study. Yihan Sun reviewed and edited the article, curated the data, contributed to software, and investigated the study. Fengxia Chi contributed to funding acquisition and supervised the study. Qinling Cheng contributed to software and validated and investigated the study. Bo Han curated the data and contributed to software.

Acknowledgments

The work described in this paper was supported by the Special Funds supported by Research Institutes in Zhejiang Province (no. 202003) and Science and Technology Program Projects (no. 2021013) of Zhejiang Provincial Department of Transportation.

References

[1] D. Han, G. Liu, Y. Xi, Y. Zhao, and D. Tang, "Performance prediction of asphalt mixture based on dynamic reconstruction of heterogeneous microstructure," *Powder Technology*, vol. 392, pp. 356–366, 2021.

[2] S. A. Ghanoon and J. Tanzadeh, "Laboratory evaluation of nano-silica modification on rutting resistance of asphalt binder," *Construction and Building Materials*, vol. 223, pp. 1074–1082, 2019.

[3] N. Kamoto, J. Govha, G. Danha, T. Mamvura, and E. Muzenda, "Production of modified bitumen from used engine oil, coal tar and waste tyre for construction applications," *South African Journal of Chemical Engineering*, vol. 33, no. 1, pp. 67–73, 2020.

[4] C. G. Shi, X. Cai, X. Y. Yi, T. L. Wang, and J. Yang, "Fatigue crack density of asphalt binders under controlled-stress rotational shear load testing," *Construction and Building Materials*, vol. 272, Article ID 121899, 2021.

[5] Q. Liu and D. Cao, "Research on material composition and performance of porous asphalt pavement," *Journal of Materials in Civil Engineering*, vol. 21, no. 4, pp. 135–140, 2009.

[6] L. Li, H. Geng, and Y. Sun, "Simplified viscosity evaluating method of high viscosity asphalt binders," *Materials and Structures*, vol. 48, no. 7, pp. 2147–2156, 2015.

[7] D. Lesueur, *Hydrated Lime: A Proven Additive for Durable Asphalt Pavements–Critical Literature Review*, Brussels: European Lime Association (EuLA) Ed, Brussels, Belgium, 2010.

[8] S. Bouron, F. Hammoum, H. Ruat, P. Métais, and D. Lesueur, "Improving the durability of asphalt mixtures with hydrated lime: field results from highway A84," *Case Studies in Construction Materials*, vol. 14, Article ID e00551, 2021.

[9] D. Lesueur, J. Petit, and H.-J. Ritter, "The mechanisms of hydrated lime modification of asphalt mixtures: a state-of-the-art review," *Road Materials and Pavement Design*, vol. 14, no. 1, pp. 1–16, 2013.

[10] P. E. Sebaaly, J. A. Epps, and D. N. Little, *The Benefits of Hydrated Lime in Hot Mix Asphalt*, National Lime Association, Arlington, VA, USA, 2001.

[11] A. K. Das and D. Singh, "Investigation of rutting, fracture and thermal cracking behavior of asphalt mastic containing basalt and hydrated lime fillers," *Construction and Building Materials*, vol. 141, pp. 442–452, 2017.

[12] Y. Niazi and M. Jalili, "Effect of Portland cement and lime additives on properties of cold in-place recycled mixtures with asphalt emulsion," *Construction and Building Materials*, vol. 23, no. 3, pp. 1338–1343, 2009.

[13] G. H. Hamedi and F. Moghadas Nejad, "Use of aggregate nanocoating to decrease moisture damage of hot mix asphalt," *Road Materials and Pavement Design*, vol. 17, no. 1, pp. 32–51, 2016.

[14] H. Behbahani, G. H. Hamedi, and V. N. M. Gilani, "Predictive model of modified asphalt mixtures with nano hydrated lime to increase resistance to moisture and fatigue damages by the use of deicing agents," *Construction and Building Materials*, vol. 265, Article ID 120353, 2020.

[15] V. N. M. Gilani, S. M. Hosseinian, H. Behbahani, and G. H. Hamedi, "Prediction and pareto-based multi-objective optimization of moisture and fatigue damages of asphalt mixtures modified with nano hydrated lime," *Construction and Building Materials*, vol. 261, Article ID 120509, 2020.

[16] H. Taherkhani and M. Tajdini, "Comparing the effects of nano-silica and hydrated lime on the properties of asphalt concrete," *Construction and Building Materials*, vol. 218, pp. 308–315, 2019.

[17] M. Ameri, M. Vamegh, S. F. Chavoshian Naeni, and M. Molayem, "Moisture susceptibility evaluation of asphalt mixtures containing Evonik, Zycotherm and hydrated lime," *Construction and Building Materials*, vol. 165, pp. 958–965, 2018.

[18] S. Han, S. Dong, M. Liu, X. Han, and Y. Liu, "Study on improvement of asphalt adhesion by hydrated lime based on surface free energy method," *Construction and Building Materials*, vol. 227, Article ID 116794, 2019.

[19] S. Han, S. Dong, Y. Yin, M. Liu, and Y. Liu, "Study on the effect of hydrated lime content and fineness on asphalt properties," *Construction and Building Materials*, vol. 244, Article ID 118379, 2020.

[20] D. N. Little and J. C. Petersen, "Unique effects of hydrated lime filler on the performance-related properties of asphalt cements: physical and chemical interactions revisited," *Journal of Materials in Civil Engineering*, vol. 17, no. 2, pp. 207–218, 2005.

[21] V. Mouillet, D. Séjourné, V. Delmotte, H.-J. Ritter, and D. Lesueur, "Method of quantification of hydrated lime in asphalt mixtures," *Construction and Building Materials*, vol. 68, pp. 348–354, 2014.

[22] D. Lesueur, J. Petit, and H. J. Ritter, "Increasing the durability of asphalt mixtures by hydrated lime addition: what evidence?" *European Roads Review*, vol. 20, pp. 48–55, 2012.

[23] A. Rasouli, A. Kavussi, M. J. Qazizadeh, and A. H. Taghikhani, "Evaluating the effect of laboratory aging on fatigue behavior of asphalt mixtures containing hydrated lime," *Construction and Building Materials*, vol. 164, pp. 655–662, 2018.

[24] C. V. Phan, H. Di Benedetto, C. Sauzéat et al., "Complex modulus and fatigue resistance of bituminous mixtures containing hydrated lime," *Construction and Building Materials*, vol. 139, pp. 24–33, 2017.

[25] S. Y. Zhu, M. Zang, M. H. Liao, and X. T. Zhu, "Analysis of viscoelastic mechanical behavior of high viscosity modified asphalt mortar," *Science Technology and Engineering*, vol. 536, no. 31, pp. 348–353, 2020, in Chinese.

[26] M. L. Xing, Z. Z. Li, R. He, X. S. Mao, Y. Zhou, and O. F. Chen, "Dynamic shear rheological properties of high viscosity asphalt mortar," *Journal of Materials Science and Engineering*, vol. 34, no. 4, 2016, in Chinese.

[27] D. C. Mo, W. D. Huang, and H. J. Zhang, "Study on the influence of filler type on asphalt mortar performance," *Petroleum Asphalt*, vol. 34, no. 2, pp. 11–15, 2020, in Chinese.

[28] Jtg e20-2011, *Standard Test Methods of Bitumen and Bituminous Mixtures for Highway Engineering*, Ministry of Transport of the People's Republic of China, SAC, Beijing, China, 2011.

[29] Gb/t 30516-2014, *High Viscosity and High Elasticity Road Asphalt*, National Standardization Administration of the People's Republic of China, SAC, Beijing, China, 2014.

[30] Aashto t350-14, *Multiple Stress Creep Recovery (MSCR) Test of Asphalt Binder Using a Dynamic Shear Rheometer (DSR)*, American Association of State and Highway Transportation Officials, Washington, DC, USA, 2015.

[31] Astm d7405-15, *Standard Test Method for Multiple Stress Creep and Recovery (MSCR) of Asphalt Binder Using a Dynamic Shear Rheometer*, ASTM International, West Conshohocken, PA, USA, 2015.

[32] J. Zhang, P. Li, M. Liang, H. Jiang, and S. Yu, "Utilization of red mud as an alternative mineral filler in asphalt mastics to replace natural limestone powder," *Construction and Building Materials*, vol. 237, Article ID 117821, 2020.

[33] J. Yu, M. Vaidya, G. Su, S. Adhikari, and S. Shekhovtsova, "Experimental study of soda lignin powder as an asphalt modifier for a sustainable pavement material," *Construction and Building Materials*, vol. 298, no. 3, Article ID 123884, 2021.

[34] A. F. Faheem and H. U. Bahia, "Conceptual phenomenological model for interaction of asphalt binders with mineral fillers," *Asphalt Paving Technology: Association of Asphalt Paving Technologists-Proceedings of the Technical Sessions*, vol. 78, pp. 679–719, 2009.

[35] A. K. Das and D. Singh, "Evaluation of fatigue performance of asphalt mastics composed of nano hydrated lime filler," *Construction and Building Materials*, vol. 269, no. 3, 2020.

[36] K. Yan, M. Zhang, L. You, S. Wu, and H. Ji, "Performance and optimization of castor beans-based bio-asphalt and european rock-asphalt modified asphalt binder," *Construction and Building Materials*, vol. 240, Article ID 117951, 2020.

[37] S. Lv, L. Hu, C. Xia et al., "Surface-treated fish scale powder with silane coupling agent in asphalt for performance improvement: conventional properties, rheology, and morphology," *Journal of Cleaner Production*, vol. 311, Article ID 127772, 2021.